NANO | MICRO

small

Supporting Information

Isolation and Profiling of Circulating Tumor-Associated Exosomes Using Extracellular Vesicular Lipid–Protein Binding Affinity Based Microfluidic Device

Yoon-Tae Kang, Emma Purcell, Colin Palacios-Rolston, Ting-Wen Lo, Nithya Ramnath, Shruti Jolly, and Sunitha Nagrath*

Supporting Information

Isolation and profiling of circulating tumor-associated exosomes using extracellular vesicular lipid-protein binding affinity based Microfluidic device

Yoon-Tae Kang[1], Emma Purcell[1], Colin Palacios-Rolston[1], Ting-Wen Lo[1], Nithya Ramnath[2], Shruti Jolly[3] and Sunitha Nagrath[1]

[1]Dr. Yoon-Tae Kang, Emma Purcell, Colin Palacios-Rolston, Ting-Wen Lo, Prof. Sunitha Nagrath
Department of Chemical Engineering and Biointerface Institute, University of Michigan, 2800 Plymouth Road, NCRC B10-A184, Ann Arbor, MI 48109, USA
E-mail: snagrath@umich.edu

[2]Dr. Nithya Ramnath
Department of Internal Medicine, University of Michigan, Ann Arbor, MI 48109, USA

[3]Dr. Shruti Jolly
Radiation of Oncology, University of Hospital, University of Michigan, 1500 E Medical Center Dr. Ann Arbor, MI 48109, USA

Keywords: Exosome isolation, cancer-associated exosome, extracellular vesicles, microfluidics, lung cancer, melanoma
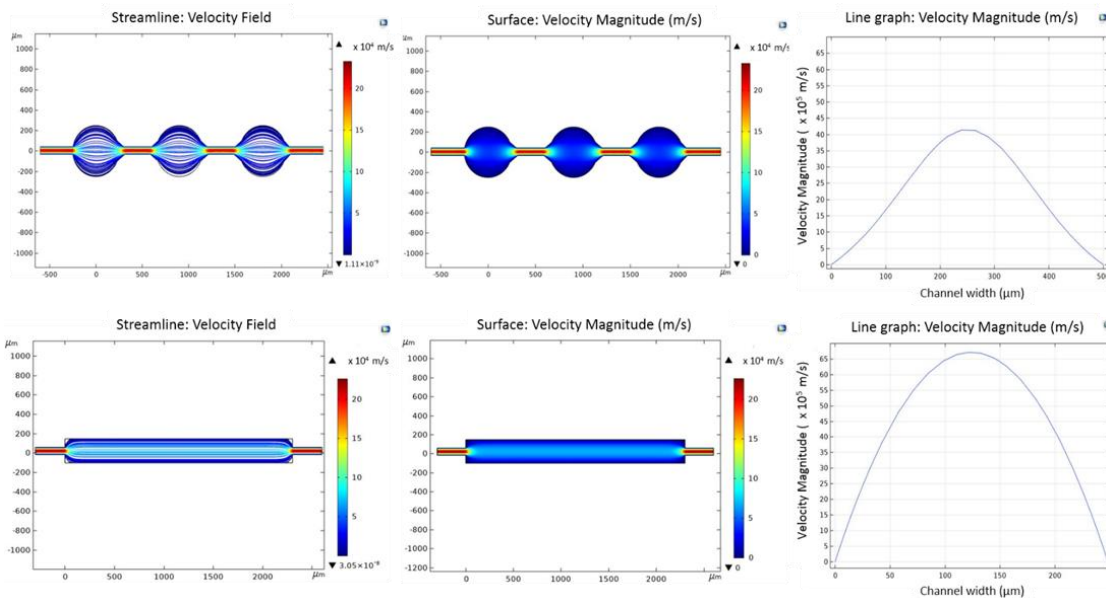
Contents

Figures & Table

**S1. Velocity profile of the circular channel in ^newExoChip**

Figure S1. Velocity profile of plasma flowing through ^newExoChip and straight channel devices

Subsections of two different devices were created in COMSOL using the laminar flow physics. The first device contains three chambers of the ^newExoChip and the second is a straight channel with the same volume as the above portion of the ^newExoChip. The devices had an inlet flow of 600uL/hr (operating flow rate of the ^newExoChip) and used laminar inflow for the boundary condition of the inlet. The walls have a no-slip condition and the outlet is set to atmospheric pressure. The overall flow patterns can be seen in the streamline and surface velocity plots, which demonstrate uniform flow in the straight channel device and slower flow in the chambers of the ^newExoChip device. As shown in the velocity line graphs, the straight channel device has a higher flowrate down the middle of the device whereas the chambers of the ^newExoChip have a markedly slower flow. This decreased flowrate enhances exosome binding affinity. Additionally, the surface area of the ^newExoChip is higher than the straight channel equivalent, allowing for again higher exosome binding.
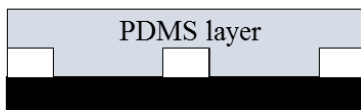
S2. Fabrication Procedure of ^newExoChip

(a) SU8 spin coating on Si wafer

SU-8 — 36μm
Si wafer
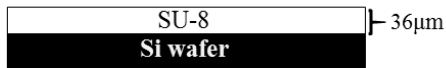
(b) UV exposure and development

(c) PDMS molding & curing

PDMS layer

(d) Peeling off the PDMS layer

PDMS Layer

(e) O$_2$ plasma bonding

PDMS Layer

Glass Slide — O$_2$ Plasma treatment
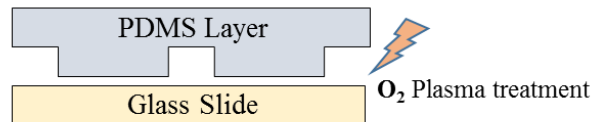
(f) Exosome-specific antibody immobilization

PDMS Layer

Glass Slide — Annexin V / PDMS/GLASS
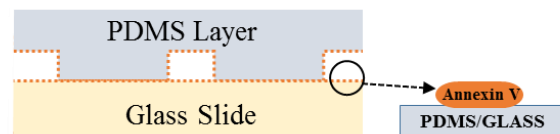
Figure S2. Fabrication and modification procedure of the ^newExoChip

The mold for the present device was fabricated by patterning SU8-2100 photoresist on a silicon wafer (a). The patterns were oppositely duplicated to the polydimethylsiloxane (PDMS) blocks by a conventional micro-molding process (c) followed by a curing process (d). As a result, the PDMS top layer was fabricated. The bonding between the PDMS layer and glass slide was done after O$_2$ plasma treatment (e). Then, the immobilization of biotinylated Annexin V proteins in the device was achieved following functionalization with the crosslinking chemistry and avidin-biotin chemistry (f).

S3. Avidin-functionalization of ᴺᵉʷExoChip
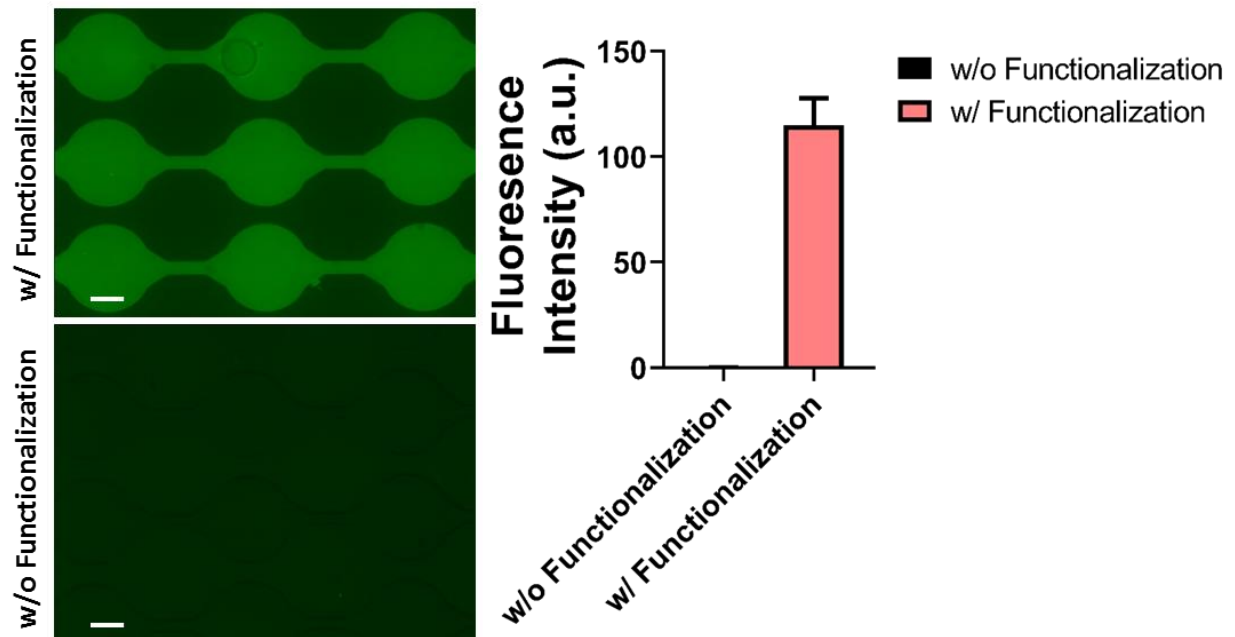
Figure S3. Staining of avidin-conjugated ᴺᵉʷExoChip by using biotinylated dye (Scale bar=200μm)

NeutrAvidin was conjugated to the ᴺᵉʷExoChip surface by means of silane and GMBS crosslinker functionalization. In order to verify the successful conjugation of NeutrAvidin to the device, we ran experiments flowing biotinylated dye through devices both with and without avidin functionalization. The images captured under the fluorescence microscope showed evenly expressed fluorescence only in the device functionalized with NeutrAvidin, indicating that the NeutrAvidin was successfully functionalized to the device and the whole device could specifically capture biotin conjugated molecules- i.e. the Annexin V used in practice.

S4. DiO staining of exosomes

	FITC	PE
A549 Exosome		
RPMI media		
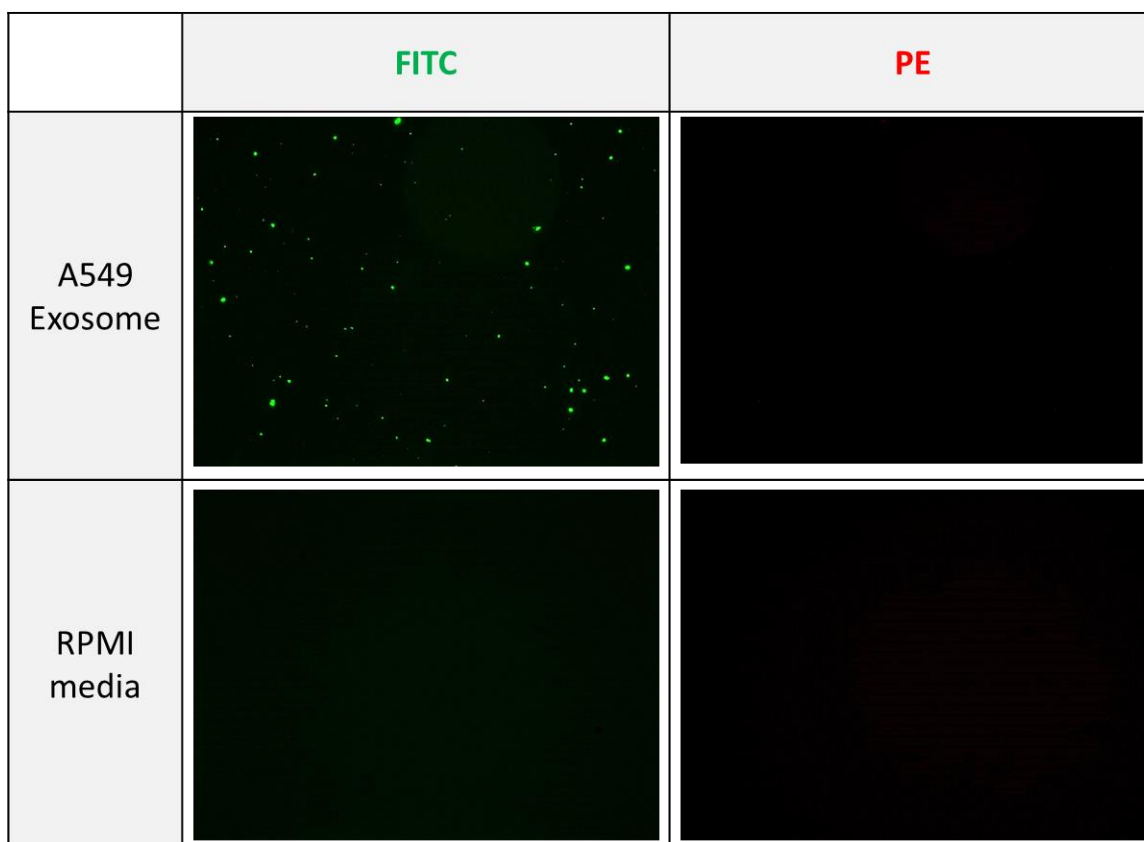
Figure S4. Confirmation of DiO stained extracellular vesicles from A549

S5. Binding affinity between Annexin V and A549 exosomes

a) Small PDMS block experiment (static)
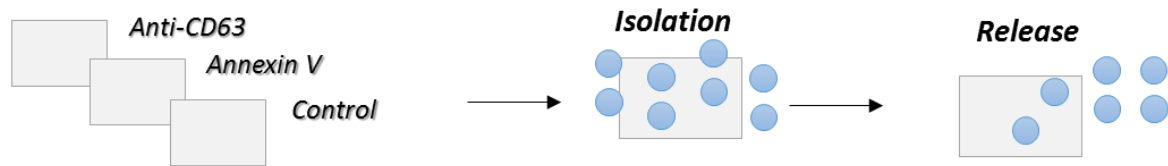
b) Small chamber device experiment (static)
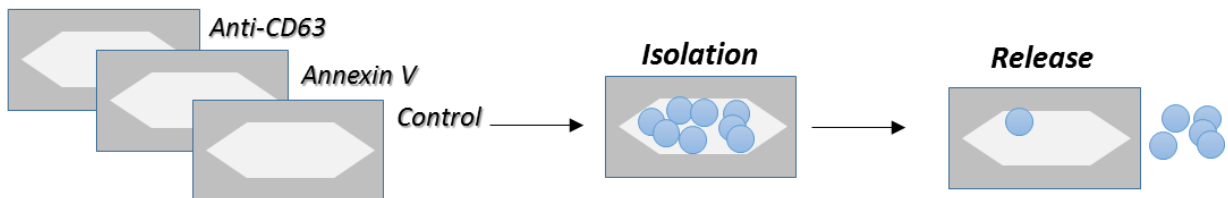
c) Small chamber device experiment (dynamic)
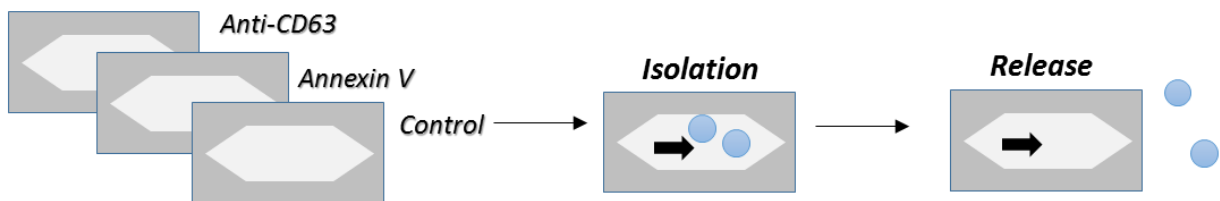
Figure S5. Binding affinity experiments using PDMS blocks and small chamber devices

For initial confirmation of the binding affinity between exosomes and Av without device optimizations (sample flow rate, incubation time, etc), we prepared a square PDMS block (10mm x 10mm) and a small chamber device (10mmx20mm) that we functionalized using biotinylated Av. For positive and negative control devices, we prepared two additional devices-one with anti-CD63 conjugation and without any antibody conjugation. Purified exosomes from the lung cancer cell line A549 were DiO stained, confirmed, and used as the exosome model sample to facilitate quick and easy validation of capture. From the small PDMS block experiments in static conditions,

we found that the Av-conjugated block captures a considerable number of exosomes after a 16 hour incubation at 4°C. The number of captured exosomes was higher using Av than with anti-CD63, with negative control devices showing negligible amount of bound exosomes. We also confirmed our ability to release exosomes using EDTA preserved washing solution. Under static condition, we applied an excess amount of 20mM EDTA to the block, performed a washing step, and evaluated for fluorescence to verify DiO-stained exosome release. After this procedure, we saw that almost all the bound exosomes had been removed from the device. We repeated the same experiments using a shorter incubation time for exosome binding and lower EDTA concentration for release and observed similar results. After these experiments, we extended our study to dynamic sample flowing through the same small chamber device. Despite the number of captured exosomes being lower in the flowing condition than the static condition, our new Av-conjugated devices were capable of exosome isolation and release, and their capturing ability was even greater compared with anti-CD63 conjugated devices.

S6. Evaluation Criteria for ^{new}ExoChip and Definitions

Capture efficiency is defined as the fraction of the isolated exosomes by ^{new}ExoChip compared to initial number of spiked exosomes. In this research, we evaluated the number of isolated exosomes by subtracting the number of exosomes in the effluent from the initial quantity. From the bulk, we only evaluated the number of exosome like vesicles, ranging 30-150nm, and it is calculated as follow.

Capture Efficiency (%)

$$= \left[1 - \frac{(Concentration\ of\ Exosome - sized\ Vesicles\ in\ Capture\ Effluent)}{(Concentration\ of\ Exosome - sized\ Vesicles\ in\ Initial\ Sample)} \right] * 100$$

Release efficiency is defined as the fraction of the released exosomes from the ^{new}ExoChip compared to the number of isolated exosomes. To evaluate this, we additionally measured the concentration of released sample after Ca^{2+} chelation, and compared this concentration to the number of isolated exosomes, which has been calculated by 'Initial exosome concentration-capture effluent's exosome concentration'. Thus, release efficiency is calculated as follow.

Release Efficiency (%)

$$= \left[\frac{(Concentration\ of\ Exosomes\ in\ Release\ Resultant)}{(Con.\ of\ Exosomes\ in\ Initial - Con.\ of\ Exosomes\ in\ Capture\ Effluent)} \right] * 100$$

In order to evaluate whether the present device captures purified exosomes from heterogeneous samples, we calculated the specificity as being the fraction of exosome sized vesicles compared to

whole concentration. The whole concentrations were directly enumerated from NTA result, and the concentrations of exosome sized vesicles were re-calculated from the NTA raw data.

$$\boldsymbol{Specificity}\ (\%) = \left[\frac{(Concentration\ of\ Exosome - sized\ Vesicles\ in\ Sample)}{(Concentration\ of\ Whole\ Vesicles\ in\ Sample)}\right] * 100$$

The recovery rate is the fraction of exosomes released from the device compared to the sum of capture effluent and release resultant. If we do not know the initial concentration of sample but want to know the isolation tendency of the present device, the simpler version of capture/release efficiency is 'recovery rate' derived only from capture effluent and release resultant's concentrations. It is calculated as follow.

$$\boldsymbol{Recovery\ Rate}\ (\%)$$
$$= \left[\frac{(Concentration\ of\ Exo - sized\ Vesicles\ in\ Release\ Resultant)}{(Concentration\ of\ Exo - sized\ Vesicles\ in\ Capture\ Effluent + Release\ Resultant)}\right] * 100$$

In addition to these evaluation factors, we also analyzed the particle-size distribution (PSD), which is a list of values of a mathematical function that defines the relative number of particles present according to size. The PSD includes the particle size span width, *D10*, *D50* and *D90*, as known as three point specification or *D-value*. Specifically, those three *D-values* indicate the diameter of the particle at 10%, 50% and 90% of the cumulative distribution. For example, if *D50* is 100nm, it means that 50% of the particles in the sample from NTA are bigger than 100nm and another 50% are smaller than 100nm.
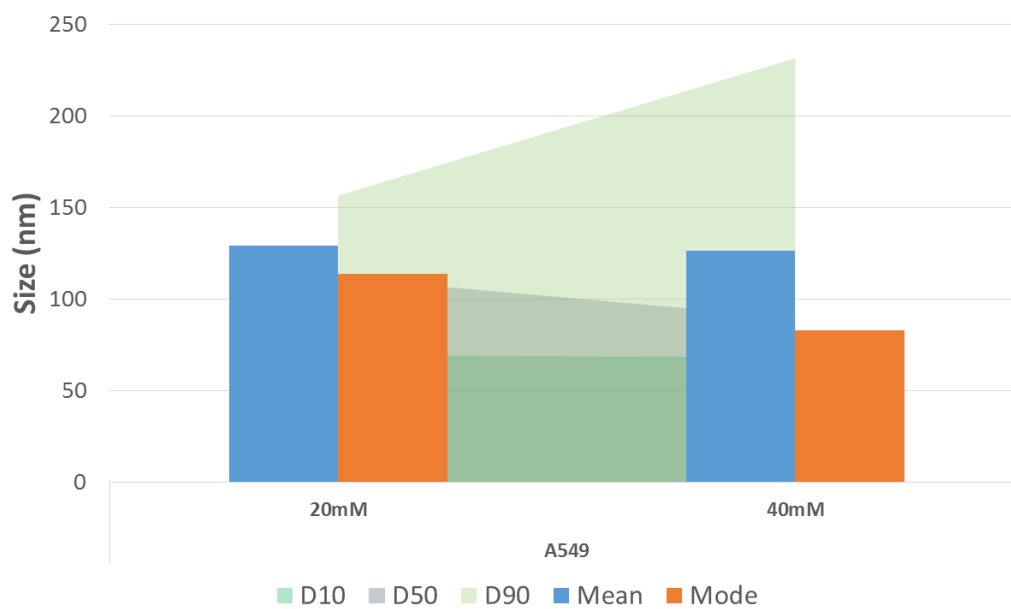
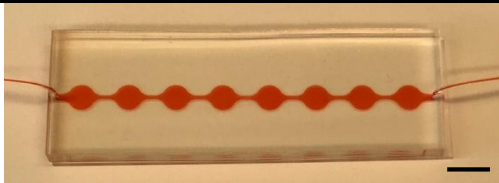**Figure S6.** Effect of 40mM EDTA treatment to exosomes

S7. Size profiling of the recovered EVs by using three different EV isolation methods
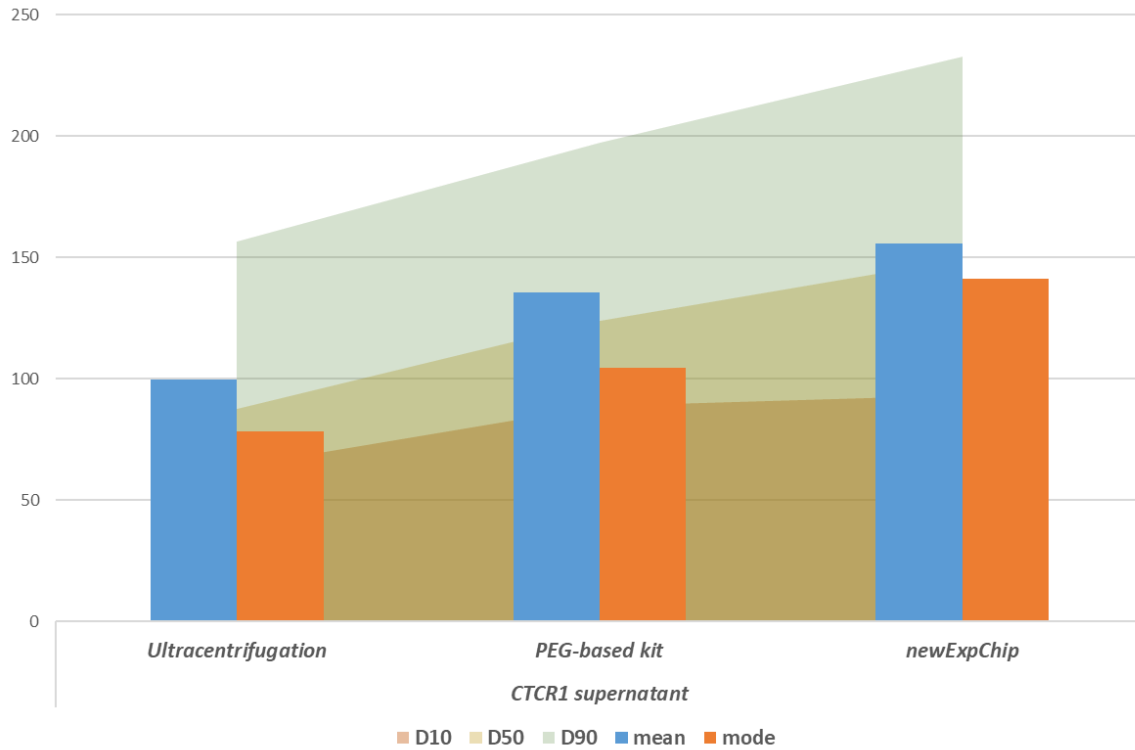
Figure S7. Size profiles of the recovered EVs by various exosome isolation methods

Table S1. The comparison table between ExoChip and ^{new}ExoChip

Scale bar=10mm

	ExoChip (2014)	^{new}ExoChip (2019)
Design	 (8x1 circular channels)	 (60x30 circular channels)
Dimension (circular channel)	75mmx25mm (diameter of 5mm)	75mmx25mm (diameter of 0.5mm)
Purpose	EV isolation/study	Exosome isolation/release/study
Principle	Immunoaffinity (tetraspanin CD63-anti-CD63)	Exosomal lipid-protein affinity (Phosphatidylserine-annexin V)
Working volume	400μl serum	>300μl serum/media
Working flow rate	0.48ml/h	>0.6ml/h
Release function	X	O
Cancer	Pancreatic	Lung, melanoma, etc.
Application	Protein, miRNA expression	Downstream analysis (protein, nucleic acids), NTA, exosome uptake experiments, etc.

S8. Isolation of immune cell derived exosomes

In order to evaluate the binding affinity between immune cell derived exosomes and Annexin V-immobilized newExoChip, we used natural killer cell line, NK92MI, as a model sample. After culture with exosome-depleted conditioned media, we performed differential centrifugation to remove cells and cellular debris followed by ultracentrifugation of the media and a known-number of exosomes were spiked into buffer solution. From those experiments, more than 90% of NK92MI-derived exosomes were recovered using our device, implying that our device has the potential to isolate immune cell-derived exosomes as well.

Table S2. The recovery rate of NK92MI derived exosomes using newExoChip

	Recovery rate
Trial 1	87.27
Trial 2	94.01
Trial 3	98.82
Average	**93.37±5.80**

Table S3. The clinical information of patients

Cancer Type	Sample ID	Sample description				
		Sex	Age	Stage	Location	Subtype
Lung cancer	*La*	M	72	IIIA	Lung	Adenocarcinoma
	Lb	M	63	IIIA	Lung	Squamous
	Lc	M	81	IIIB	Lung	Adenocarcinoma
	Ld	F	64	IIIB	Lung	Adenocarcinoma
Melanoma	*Ma*	F	-	IIIC	right central frontal scalp	-
	Mb	M	-	IIA	lateral right cheek	-
	Mc	F	-	IB	left central lateral neck	-